Electronic Supplementary Material (ESI) for Inorganic Chemistry Frontiers.

Support information

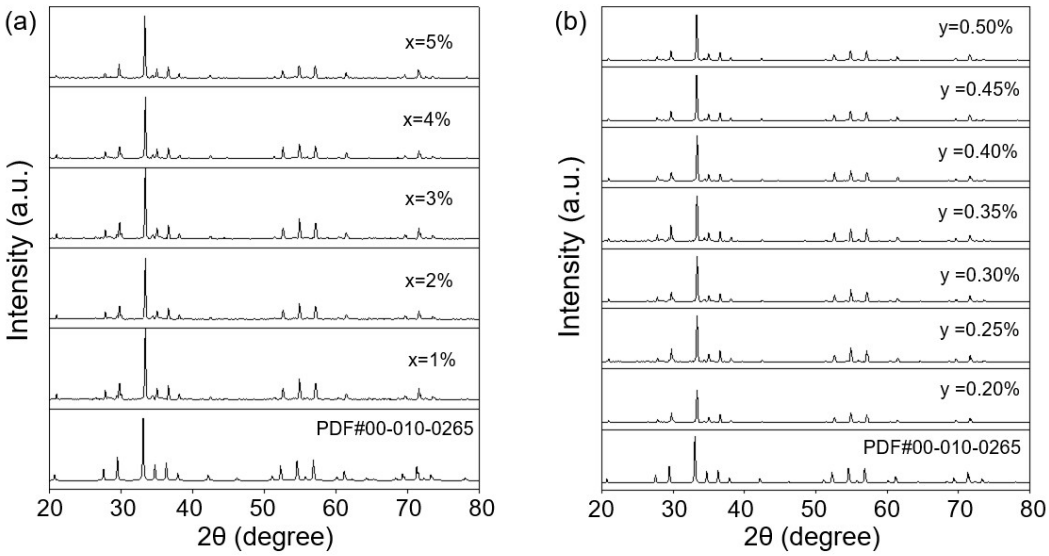

Fig.S1 (a) XRD patterns of CAG:xMn^{2+} (x=1%-5%) and CAG:2%Mn^{2+}, yCr^{3+}(y=0.2%-0.5%).

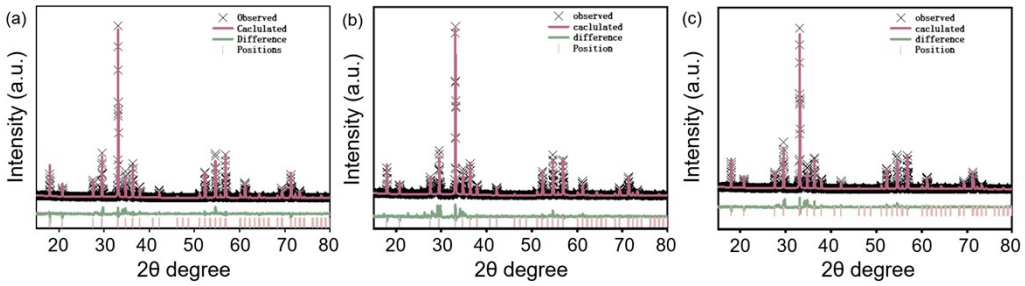

Fig.S2 The refinement XRD patterns of CAG:2%Mn^{2+}, yCr^{3+}(y=0.2%-0.4%).

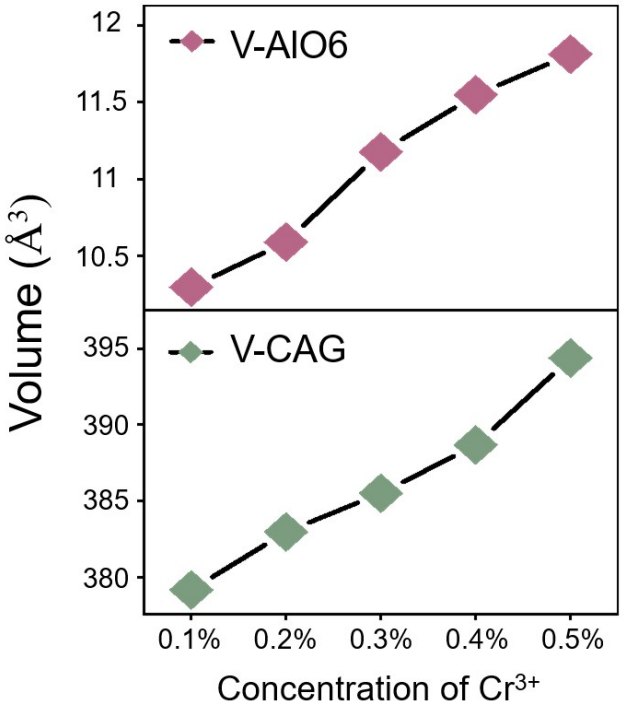

Fig.S3 Variation of lattice volume and CAG volume of AlO6.

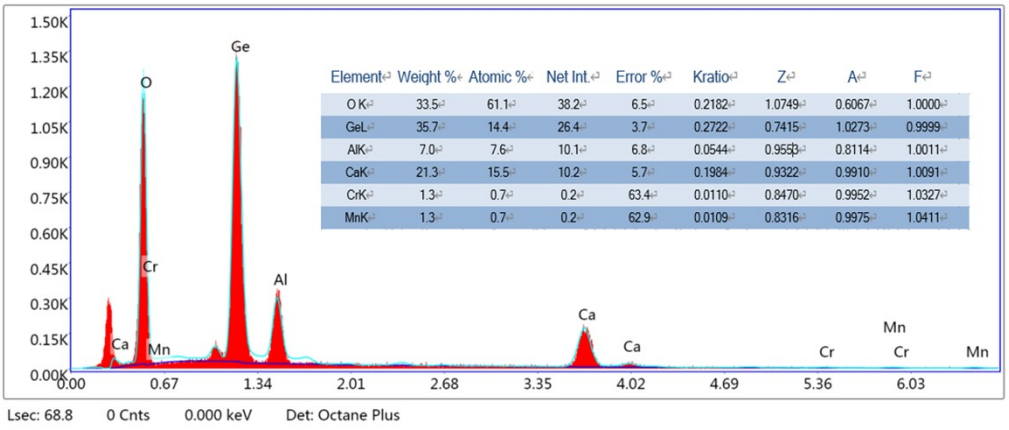

Element	Weight %	Atomic %	Net Int.	Error %	Kratio	Z	A	F
O K	33.5	61.1	38.2	6.5	0.2182	1.0749	0.6067	1.0000
GeL	35.7	14.4	26.4	3.7	0.2722	0.7415	1.0273	0.9999
AlK	7.0	7.6	10.1	6.8	0.0544	0.9553	0.8114	1.0011
CaK	21.3	15.5	10.2	5.7	0.1984	0.9322	0.9910	1.0091
CrK	1.3	0.7	0.2	63.4	0.0110	0.8470	0.9952	1.0327
MnK	1.3	0.7	0.2	62.9	0.0109	0.8316	0.9975	1.0411

Fig.S4 EDS spectrum of CAG:2%Mn^{2+}, 0.5%Cr^{3+}, inset: the weight and atomic percentage.

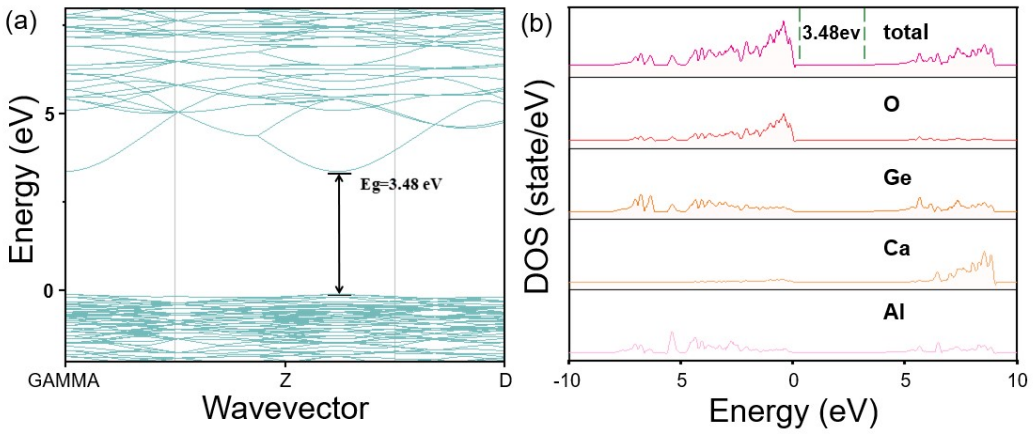

Fig.S5 (a) Calculated band structure of host CAG based on the refined crystallographic results using first principles. (b) Total density of states (TDOS) and partial density of states (PDOS) of CAG.

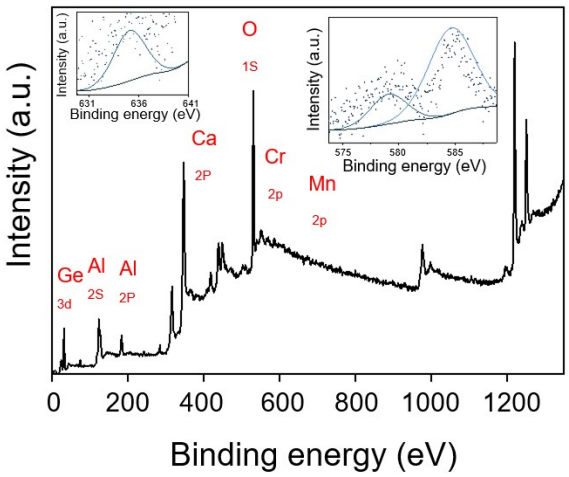

Fig.S6 XPS spectrum of CAG:2%Mn^{2+} ,0.5%Cr^{3+}; inset: the XPS spectrum of Cr^{3+} at the $^2p_{1/2}$ energy level.

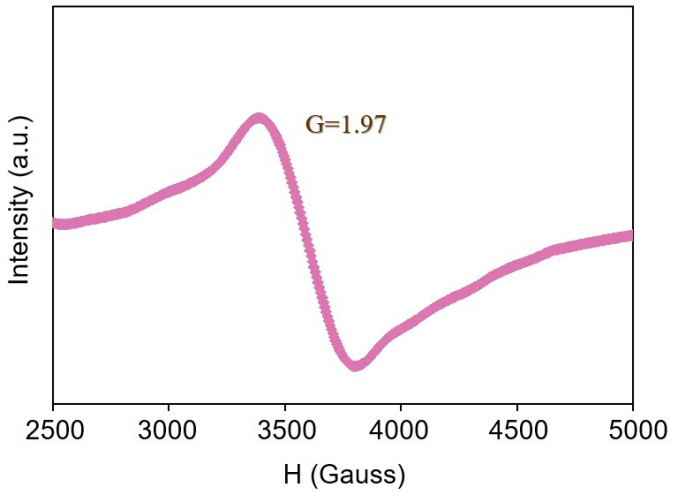

Fig.S7 EPR spectra of CAG:2%Mn^{2+}, 0.5%Cr^{3+} under UV irradiation 11min at 77 K.

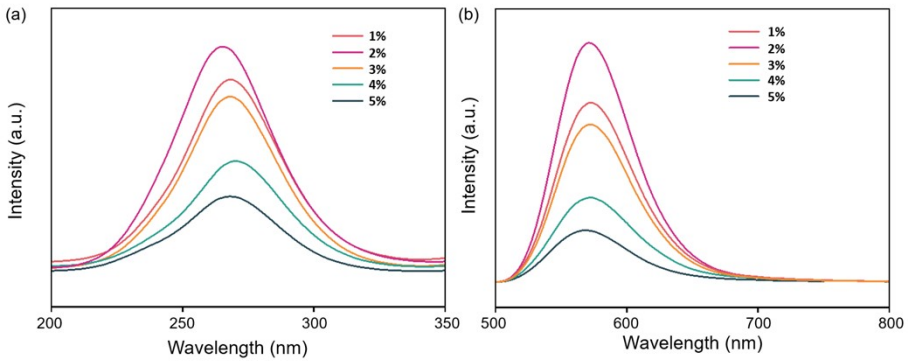

Fig.S8 (a) PLE and (b) PL spectra of CAG:$x$$Mn^{2+}$ (x=1%-5%, λ_{em} = 568 nm λ_{ex} = 265 nm).

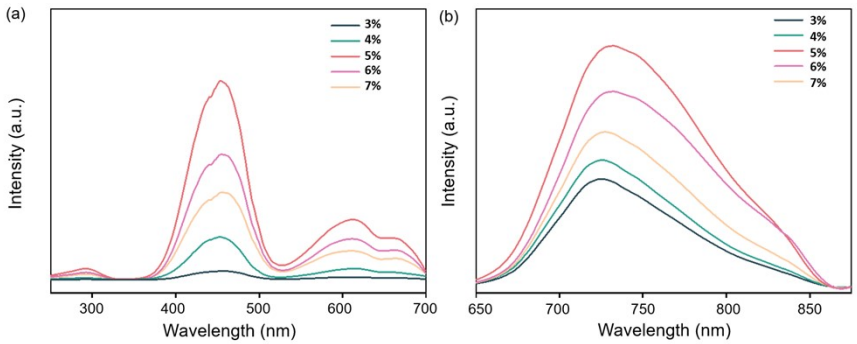

Fig.S9 (a) PLE and (b) PL spectra of CAG:$x$$Cr^{3+}$ (x=3%-7%, λ_{em} = 722nm λ_{ex} = 454nm).

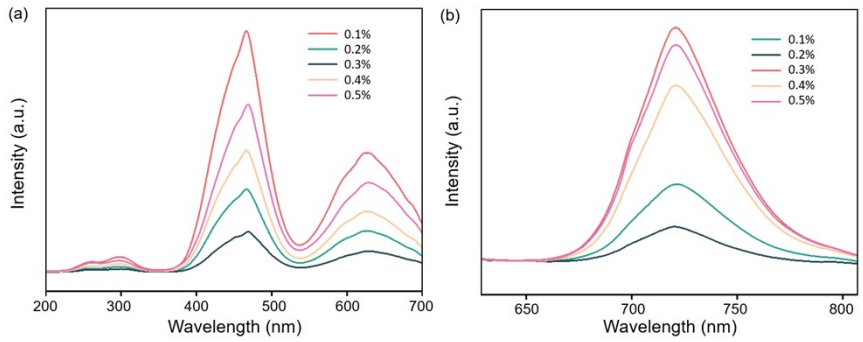

Fig.S10 (a) PLE and (b) PL spectra of CAG:2%Mn^{2+}, *y*Cr^{3+} (*y*=0.1%-0.5%, λ_{em}=722 nm, λ_{ex}=465 nm).

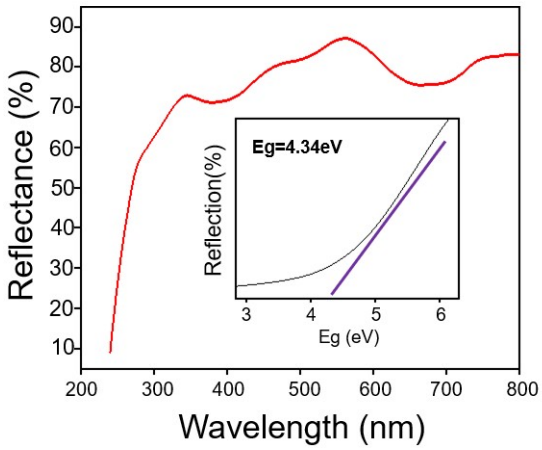

Fig.S11 The diffuse reflection spectra of CAG:2%Mn^{2+}, 0.5%Cr^{3+}; inset: the calculation and analysis result of bandgap width.

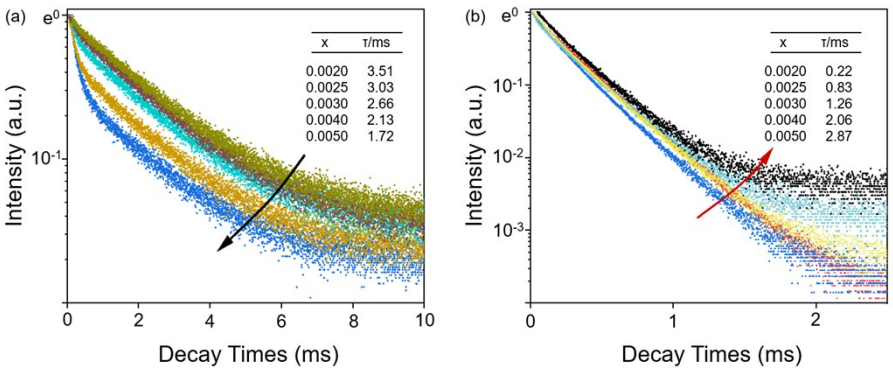

Fig.S12 (a) Decay curves of Mn^{2+} (λ_{em}=568 nm) (b) Decay curves of Cr^{3+} (λ_{em}=722 nm).

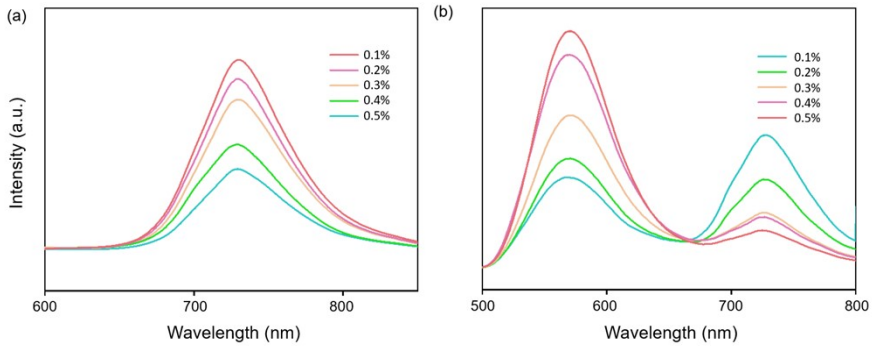

Fig.S13 PersL spectra (λ_{ex}=454 nm) (a) and (λ_{ex}=254 nm) (b).

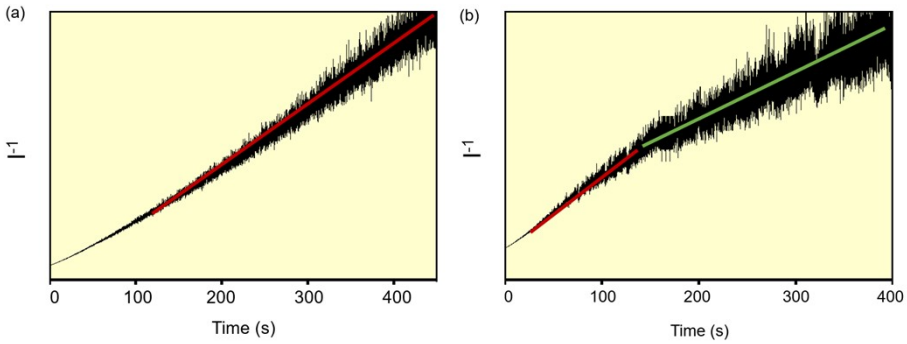

Fig. S14 The inverse of the afterglow intensity of CAG:2% Mn^{2+}, 0.5%Cr^{3+} as a function of decay time (λ_{em}=568 nm) (a) and (λ_{em}=722 nm) (b).

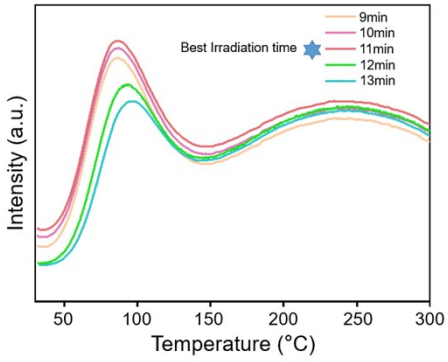

Fig. S15 The TL spectra of CAG:2%Mn^{2+}, 0.5%Cr^{3+} varies with different irradiation times.

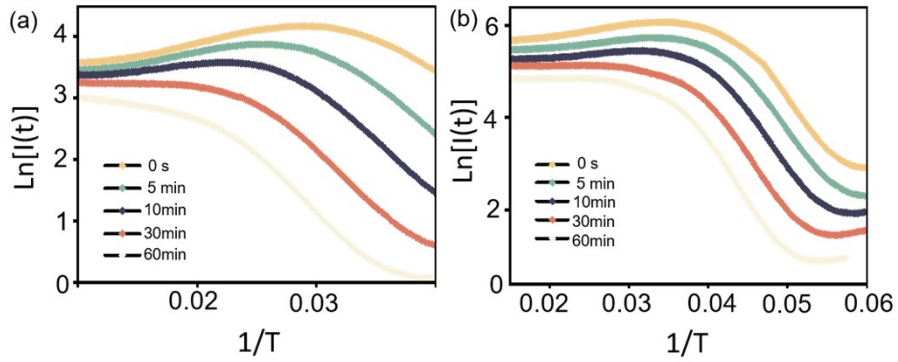

Fig. S16 The inverse of the afterglow intensity of CAG:2% Mn^{2+}, 0.5% Cr^{3+} as a function of decay time (λ_{em}=568 nm) (a) and (λ_{em}=722 nm) (b).

Table S1 Commission International de I'Eclairage (CIE) for CAG:2%Mn, *x*%Cr (*x*=0.2%,0.5%) chromaticity coordinates column at different temperatures.

Samples	X	Y
	300K	
CAG: 2% Mn^{2+}, 0.2% Cr^{3+}	0.2957	0.6122
CAG: 2% Mn^{2+}, 0.5% Cr^{3+}	0.5628	0.3714
	473K	
CAG: 2% Mn^{2+}, 0.2% Cr^{3+}	0.4211	0.2346
CAG: 2% Mn^{2+}, 0.5% Cr^{3+}	0.5754	0.3152

Note: There are two ways to calculate energy transfer efficiency --- by PL intensity and lifetime, respectively. The first one is calculated by PL intensity which is influenced merely by the ET process, the ET efficiency from Mn^{2+} to Cr^{3+}, can be calculated by[1-2]

$$\eta_{ET}=1-\frac{I_{Mn}}{I_{Mn0}} \quad \text{(S1)}$$

where I_{Mn} and I_{Mn0} were the Cr emission intensity in the absence and in the presence of Cr^{3+}. The second one is calculating by the decreases of lifetime. The ET efficiency η_{ET} from Mn^{2+} to Cr^{3+} can be calculated by the following equation[3]:

$$\eta'_{ET}=1-\frac{\tau_{Mn}}{\tau_{Mn0}} \quad \text{(S2)}$$

where τ_{Mn} represents the lifetime of Mn^{2+} with various Cr^{3+} concentration, and τ_{Mn0} is the lifetime of Mn^{2+} in Mn^{2+} single-doped sample. It may be noticed that the values calculated by Equation (S2) are apparently smaller than those calculated by Equation (S1), which may be explained by experimental error from the measurement of the spectrum. So, we use the average values of the ET efficiency.

References

1. He, S.; Zhang, L. L.; Wu, H.; Wu, H. J.; Pan, G. H.; Hao, Z. D.; Zhang, X.; Zhang, L. G.; Zhang, H.; Zhang, J. H., Efficient Super Broadband NIR $Ca_2LuZr_2Al_3O_{12}:Cr^{3+},Yb^{3+}$ Garnet Phosphor for pc-LED Light Source toward NIR Spectroscopy Applications. *Adv Opt Mater* **2020,** *8* (6), 1901684.1.

2. Basore, E. T.; Wu, H. J.; Xiao, W. G.; Zheng, G. J.; Liu, X. F.; Qiu, J. R., High-Power Broadband NIR LEDs Enabled by Highly Efficient Blue-to-NIR Conversion. *Adv Opt Mater* **2021,** *9* (7), 2001660.

3. Liu, D. J.; Li, G. G.; Dang, P. P.; Zhang, Q. Q.; Wei, Y.; Qiu, L.; Molokeev, M. S.; Lian, H. Z.; Shang, M. M.; Lin, J., Highly efficient Fe^{3+}-doped A(2)BB'O^{-6} (A = Sr^{2+}, Ca^{2+}; B, B'= In^{3+}, Sb^{5+}, Sn^{4+}) broadband near-infrared-emitting phosphors for spectroscopic analysis. *Light: Sci & Appl* **2022,** *11* (1), 969.